High Power Eye-Safe Optical Wireless Gigabit Link Employing a Freeform Multipath Lens

René Kirrbach, Michael Faulwaßer, Mira Stephan, Tobias Schneider, and Frank Deicke

***Abstract*— This work experimentally demonstrates for the first time the practical feasibility of a freeform multipath lens (MPL) for optical wireless communications (OWC). The MPL is able to increase the eye safety laser power limit. Our transmitter is laser class 1M and features 190 mW optical output. We transmit 1.289 Gbit/s on-off keying (OOK) data and achieve a bit error ratio (BER) of 10^{-10} for an optical receiver power of −31.2 dBm. The link range is more than 5 m, depending on the targeted BER. We discuss the pros and cons of MPLs and compare them with diffusers.**

***Index Terms*— Bit error ratio, eye safety, freeform optics, laser diodes, LiFi, multipath lens, optical diffusers, optical wireless communications, on-off keying.**

I. Introduction

NEW applications demand low-latency, wireless data transfer [1]. At the same time, there is a steady growth in the global mobile data traffic [2], [3], that leads to interference issues in the crowded radio-frequency spectrum. One way to achieve reliable low-latency data transfer is to use spatially confined optical wireless communication (OWC) channels.

By using laser diodes (LDs) as optical emitters, optical wireless transceivers reach data rates in the range of Gbit/s even with simple modulation schemes like on-off keying (OOK) [4], [5]. OOK enables ultra-low-latency data transfer. In contrast, transceivers with conventional light-emitting diodes (LEDs) require sophisticated modulation schemes like orthogonal frequency-division multiplexing (OFDM), which comes with higher latency. Consequently, there is a scientific interest in exploiting LDs for indoor OWC [6]–[8].

Laser light can be harmful for the human eye and skin. Therefore, the optical output for laser class 1/1M is restricted to a few milliwatts or even less, depending on the wavelength and the emission profile of the LD [9]–[11]. The power restriction limits the link range and the practical feasible field of view (FOV) size. Wide FOVs result in a large link loss, that cannot be compensated with a higher LD power. Consequently, most LD links are based on simple point-to-point architectures [5], [12].

There are several approaches to surpass the power limitations. For instance, LD arrays instead of single LDs can be employed [8], [13], [14]. Alternatively, different kinds of diffusers might be used [6], [15], [16]. A promising alternative for visible light communications (VLC) is the use of phosphor or remote phosphor [6], [17], [18]. It scatters the light like a diffuser and acts as a color converter to generate white light. All of these methods come with several drawbacks, e.g., the scatter-based approaches suffer from reduced efficiency for small FOVs and low flexibility in terms of FOV shape. A recent work describes an alternative approach: a freeform multipath lens (MPL) that allows precise control over the emission profile, overcomes the common laser power restrictions [19], and can be fabricated in a high-volume injection molding process. The work describes the optical design aspects, including the geometrical design procedure, ray-tracing simulations, and optical power measurements. However, data transfer experiments were out of the scope.

In this work, an MPL is implemented in an optical wireless transceiver and data transfer experiments are carried out. For the first time, we prove the practical feasibility of the MPL for LD-based OWC. Bit error ratio (BER) measurements show a range of more than 5 m, depending on the required BER. Moreover, we discuss the pros and the cons of MPLs for OWC and compare them with other approaches like diffusers and LD arrays.

The letter is organized as follows. Chapter II gives a short overview of MPL fundamentals. In chapter III, we describe the experimental setup. The measurement results are presented in chapter IV and discussed in chapter V. Chapter VI provides a summary.

II. Multipath Lens Fundamentals

A. Eye Safety

The following paragraphs describe the working principle of the MPL in a short form. A detailed description of the eye safety regulations and the analytical definitions can be found in IEC 60825-1:2014 [10] and in a tutorial of Soltani *et al.* [11].

The MPL is a faceted lens, but not just a simple lens array with identical elements. Instead, each facet is a freeform surface that shapes an individual sub-spot. All sub-spots superimpose and form the overall transmitter (TX) spot. It increases the allowed laser power Φ_{TX} by means of two effects: (1) the reduction of incident power Φ_{det} and (2) the increase of the maximum permissible exposure (MPE) by enlarging the angular subtense α of the *apparent source*. Φ_{det} is the power measured within the laser class measurement setup that is defined by IEC 60825-1:2014 [10]. Thereby, the detector represents the retina of the human eye. The MPE is the limit that must not be exceeded for the corresponding laser class.

Manuscript received March 1, 2022; accepted March 18, 2022. Date of publication March 28, 2022; date of current version June 10, 2022. The associate editor coordinating the review of this letter and approving it for publication was O. Amin. *(Corresponding author: René Kirrbach.)*

The authors are with the Fraunhofer IPMS, 01109 Dresden, Germany (e-mail: rene.kirrbach@ipms.fraunhofer.de).

Digital Object Identifier 10.1109/LCOMM.2022.3162642

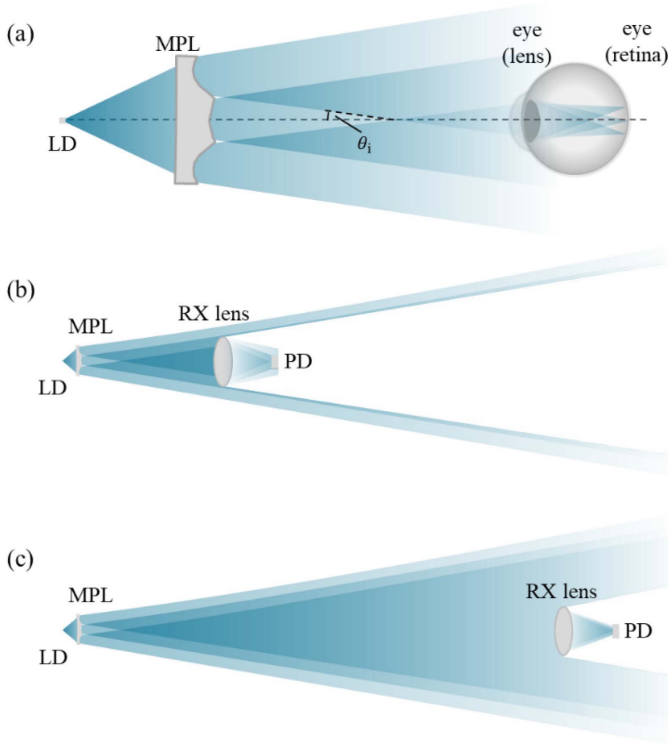

Fig. 1. (a) Close-up: focused light at the human eye for nearby transmitter (TX); (b) Long shot: focused light at a receiver (RX) close to TX; (c) Long shot: focused light at RX in large distance.

The MPE of a laser class depends on the size of the apparent source, which is quantified with the angular subtense α. α is a measure of the angular extent of the image formed on the retina [16]. In other words, the angular subtense α indicates how sharply light is focused onto the retina. A small α refers to a small image and a high power density. Consequently, the MPE is low. A laser source typically exhibits $\alpha \leq 1.5\,\text{mrad}$, which is considered a *point source* [10].

The MPL is able to increase α. Fig. 1 (a) shows that the light from the MPL is not focused on a single point on the retina. Instead, each illuminated facet is focused on a different point of the retina due to the relative position of each facet corresponding to the eye's lens. Thus, the angle of incidence θ_i is different. The off-axis facets lead to oblique irradiation and form off-axis focus points. Thereby, the power spreads over the retina, which refers to a larger α and an increased MPE. The number of facets and focus points is in the range of $10^1 \ldots 10^4$. In practice, the number of facets is limited by their size and the resolution of the fabrication technology.

Determining the MPE and the laser class of a system requires a measurement according to IEC 60825-1:2014 [10] or at least an adequate simulation model. It is difficult to calculate the MPE directly since it depends not only on the MPL size but also on the LD's emission profile, the overall MPL shape, the facet shape, the number of facets, and the receiving lens.

Nevertheless, the Étendue can be used to show the basic relationships. The conservation of Étendue limits the focus point's minimum size and thereby the angular subtense α. The Étendue of a ray bundle is proportional to its spatial and its angular extent [20, pp. 18-22]. Increasing the spatial and angular extent by scaling up the MPL size and the emission angle will increase the MPE. From Fig. 1 (a) it is clear that both approaches increase the maximum θ_i and the image size. A larger α leads to a higher MPE.

B. Optical Wireless Communications

Fig. 1 (b) and Fig. 1 (c) illustrate the light paths at an optical receiver in close and long proximity. It can be seen how the sub-spots of every facet superimpose to the TX spot. For a receiver at a long distance, the relative position of the facets in relation to the receiver (RX) lens is very similar. Consequently, all facets are similarly focused on the PD. In close proximity, a certain part of the light misses the PD due to two effects. (i) The eye covers a larger solid angle in front of each facet. The larger divergence of the ray bundles increases the focus point size. This effect applies also to conventional TX lenses. (ii) The incident angle of the off-axis facets is larger. Therefore, their focus point moves away from the PD center. Both effects reduce the receiver power in close proximity and can help to avoid receiver saturation.

III. Experimental Setup

Fig. 2 shows the x-alignment setup for the sensitivity measurement, the bit error rate test (BERT), and the eye diagram measurement. The TX and the RX board are mounted on precision X-Y-Z stages in front of each other at a distance of $z_0 = 0.95$ m. The channel loss is adjusted by varying the displacement along the X-axis. A front plate with the MPL is mounted right in front of the TX. The boards are stacked on supply boards, which provide the supply voltage and differential *SubMiniature version A* (SMA) inputs and outputs. The inlet in Fig. 2 (a) shows a front image of the active transmitter. The camera lens focuses the light from each facet onto a different set of camera pixels.

Fig. 2 (b) illustrates the measurement setup schematically. A *Stratix V* FPGA board generates a pseudo-random bit sequence (PRBS-7). The FPGA feeds the signal into the TX. A custom laser driver drives the LD accordingly. The MPL directs the emitted light. A custom total internal reflection (TIR) receiver lens with an input diameter of 8.8 mm concentrates the incident light onto the avalanche photodiode (APD). The APD diameter is 0.5 mm. The photodiode (PD) converts the optical signal into a photocurrent. The transimpedance amplifier (TIA) transforms the photocurrent into a voltage signal. The FPGA samples the signal and carries out the BERT to evaluate the signal performance. To determine the optical input power $\Phi_{\text{RX DC}}$, we measure the photocurrent and use the APD responsivity to convert it. For the photocurrent measurements, we temporally deactivate the APD bias to avoid corruption by the APD's avalanche effect. The oscilloscope *Lecroy 10-36Zi* samples the TIA output and generates the eye diagrams. The active probe *DH25* provides a bandwidth of 13 GHz.

Within a 2nd experiment, we place the devices on the ground and measure the BERT over the z-alignment. To avoid long

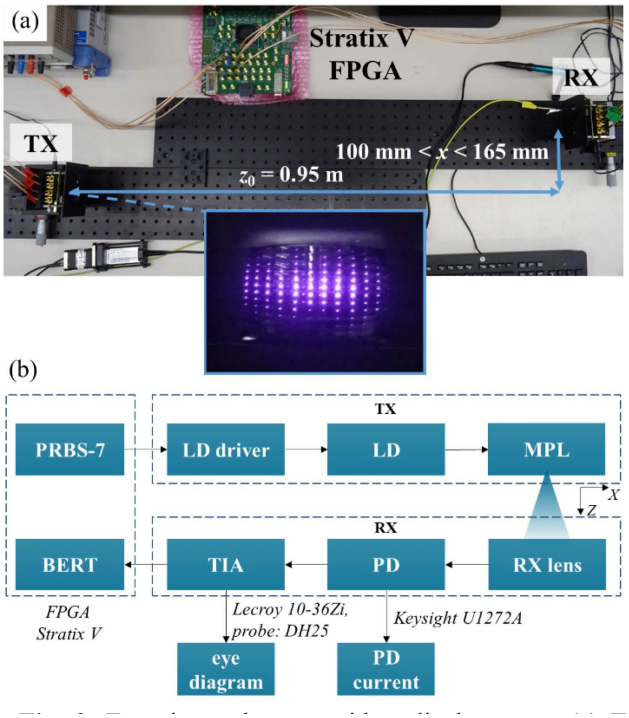

Fig. 2. Experimental setup with x-displacement. (a) Top view with illuminated MPL (inlet). (b) Schematic illustration.

wires in the experiment, we use two identical FPGAs, one for the PRBS generation at the TX and one for the BERT at RX.

Table I summarizes the parameters of the optical wireless link. For the BERT, we transmit non-return-to-zero (NRZ) on-off keying (OOK) signals with a symbol rate of 1.289 Gbit/s. We choose this data rate since it is relevant in practical applications like industrial real-time (RT) data protocols. The MPL consists of 12 × 12 individual facets. It shapes a spot with a quadratic cross-section. The emission half-angle along the X- and Y-axis is $\theta_{TX} = 7°$. The MPL increases the allowed laser class 1M power of our LD from 17.7 mW without the lens to 354 mW with the lens [19]. In our setup, the power is $\Phi_{TX\,DC} = 190$ mW. This corresponds to a margin for laser class 1M operation of 2.7 dB. It is a reasonable margin for eye safety if we consider a constant high-level output as 1st order error.

TABLE I
PARAMETERS OF THE OPTICAL WIRELESS LINK

Parameter	Symbol	Value	Unit
Bit rate	R	1.289	Gbit/s
Modulation	-	NRZ-OOK	-
LD type	-	Edge emitter	-
Wavelength	λ	850	nm
Optical power	$\Phi_{TX\,DC}$	190	mW
MPL size	$h \times w$	19 × 11	mm × mm
MPL facet count	N	12 × 12	-
TX emission angle	θ_{TX}	7	°
Laser class	-	1M	-
PD	-	Si-APD	-
PD diameter	d_{APD}	0.5	mm
RX lens diameter	d_{RX}	8.8	mm
RX lens FOV	θ_a	5	°
Full channel bandwidth	f_{-3dB}	770	MHz
Probe bandwidth	f_{probe}	13	GHz

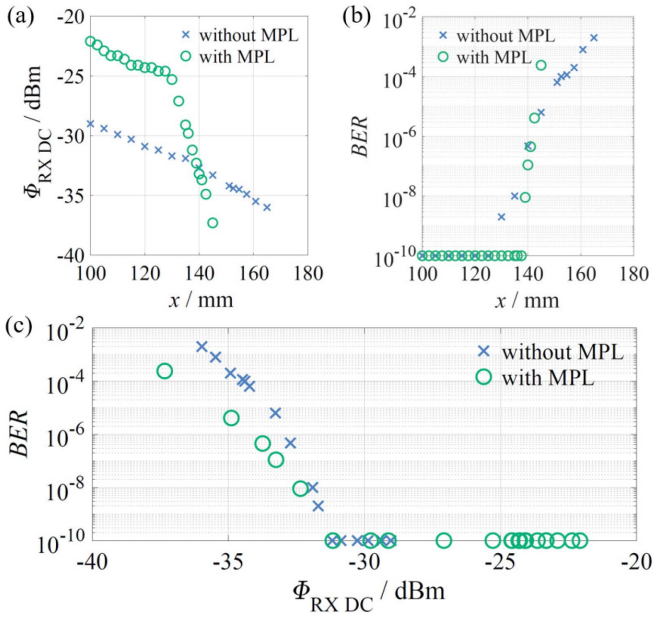

Fig. 3. Experimental results with x-displacement: (a) $\Phi_{RX\,DC}$ versus x-displacement, (b) BER versus x-displacement, (c) BER versus $\Phi_{RX\,DC}$. The BERT is clipped at 10^{-10}.

IV. MEASUREMENTS

Fig. 3 (a) and Fig. 3 (b) show the measured optical receiver power $\Phi_{RX\,DC}$ and the BER over the x-displacement. The different emission profiles with and without MPL cause the difference in $\Phi_{RX\,DC}$. Fig. 3 (c) is generated from this data by plotting the BER versus $\Phi_{RX\,DC}$. The BERT is clipped at $BER < 10^{-10}$. For strong receiver signals and low error rates, both links perform similarly. The link with the MPL achieves a $BER < 10^{-10}$ for $\Phi_{RX\,DC} \geq -31.2$ dBm. For weaker receiver signals, the MPL link outperforms the link without MPL. For instance, at $\Phi_{RX\,DC} = -35.0$ dBm the system without MPL exhibits a BER of $2 \cdot 10^{-4}$. The MPL link requires -37.3 dBm for $2.4 \cdot 10^{-4}$.

Fig. 4 (a) shows the eye diagram for $\Phi_{RX\,DC} = -24.6$dBm ($BER \ll 10^{-10}$). It is open and practically allows error-free transmission. It features a weak low-pass behavior and a weak overshoot at the high level. Both effects are caused by the non-flat frequency response of the LD driver and the TIA.

Fig. 4 (b) shows the eye diagram for $\Phi_{RX\,DC} = -33.3$ dBm ($BER = 1 \cdot 10^{-7}$). The eye is much noisier and it also exhibits the low-pass effect. The amplitudes of both eye diagrams appear to be quite similar because the APD bias voltage and thus the APD gain is adjusted in a control loop. The higher APD gain in Fig. 4 (b) leads to stronger excess noise [21, pp. 58-60]. In addition, the avalanche effect leads to higher noise at the high level compared to the low level.

Fig. 5 shows the BERT results over the z-alignment. For 1 m $< z <$ 4.5 m, the BER is $<10^{-10}$. From z = 5 m on, the BER increases steadily. At z =7.5 m, we find $BER = 6.9 \cdot 10^{-5}$.

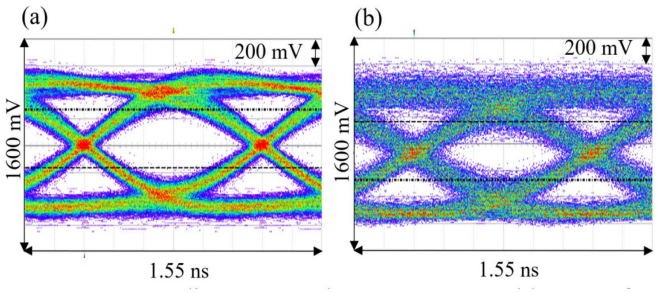

Fig. 4. Eye diagrams at the TIA output with MPL for (a) $\Phi_{\mathrm{RX\,DC}} = -24.6\,\mathrm{dBm}$ and (b) $\Phi_{\mathrm{RX\,DC}} = -33.3\,\mathrm{dBm}$. The observed bandwidth is 3 GHz.

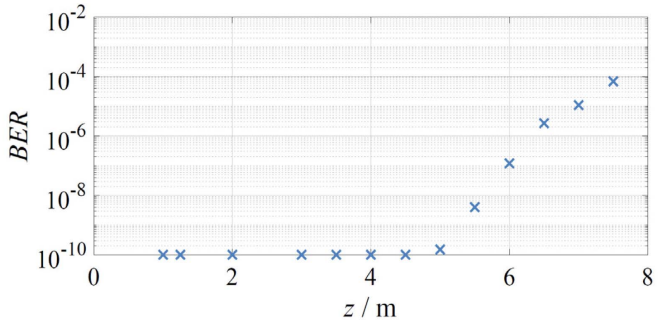

Fig. 5. BER over z-alignment with MPL (x = 0). The BERT is clipped at 10^{-10}.

V. Discussion

A. Results

The measurement results prove the feasibility of MPLs for OWC. The MPL does not degrade the transceiver's performance. In our experiments, the MPL even improves the sensitivity for BER $> 10^{-10}$. We ruled out that the effect is caused by multipath propagation by using an aperture within the optical channel, which blocks indirect light paths. We believe that the effect is caused by noise due to the Speckle of the multi-mode LD in conjunction with the TIR receiver lens. The MPL has an averaging effect because the receiver detects rays from many facets, where each ray path is slightly different. Diffusers have the same effect. Therefore, it is no MPL exclusive advantage.

The z-alignment measurement from Fig. 5 shows a range of 5 m and more, depending on the targeted BER. We can further increase the transmitter power Φ_{TX} and still maintain laser class 1/1M by scaling up the FOV or the MPL size. In addition, the inlet in Fig. 2 (a) reveals that the output power is not homogeneously distributed over the facets. Center facets feature more power than edge facets. A more homogenous distribution further improves eye safety. However, this requires an additional optical element at the transmitter. For most indoor scenarios a range of 5 m is already sufficient. Instead, the excess margin could be used to increase the FOV.

Most practical systems can use a forward error correction (FEC) to improve the transceiver's sensitivity below $-37\,\mathrm{dBm}$. In Fig. 5, this corresponds to a range of approximately z = 7.5 m. However, the introduced latency of the FEC can be critical for certain industrial RT protocols.

B. Comparison of Diffusers, MPLs, and LD Arrays

Which approach is the best to ensure eye safety in OWC? Generally, scattering-based approaches are sufficient if a very large FOV ($\approx 60°$) is required. This might be the case for full-room illumination and most non-line-of-sight (NLOS) scenarios. In the case of VLC, the remote phosphor technique is promising since it combines color conversion and diffuser functionality. If the color conversion is too slow for the signal, the available transmitter power for the link budget is reduced. The MPL and simple diffusers do not feature this limitation. MPLs are suited if a defined spot is wanted, which is typically the case for line-of-sight (LOS) scenarios. In this case, the MPL achieves a superior performance due to high efficiency and high power homogeneity compared to scatter-based solutions. There is no optical property that prevents us from using it in NLOS scenarios. However, it features no distinct benefit over diffusers if no defined FOV is required. Regardless of whether a diffuser or a lens is used, NLOS scenarios require a suitable modulation scheme to address multipath propagation.

The MPL is robust against dirt and other particles on its surface. Particles only affect the corresponding facets but do not create blind spots within the FOV. This advantage is shared with most diffuser-based approaches. The MPL is fabricated by injection molding and is suited for large-volume production. The main drawback of the MPL is the high initial effort for the optical design and the fabrication of the injection molding tool.

Only an engineered diffuser with a controlled microstructure achieves a similar performance like the MPL. Because this kind of diffuser is typically costly in fabrication, it might be a good choice for research and test setups but not for large-volume production. In addition, it typically requires an additional collimator lens.

The use of LD arrays can be understood as an additional degree of freedom since the LD array can be combined with all previous methods to increase Φ_{TX} even further. Vertical-cavity surface-emitting laser (VCSEL) arrays seem a promising candidate for practical applications [8].

For completeness, Table II shows a selection of indoor OWC links, which feature high TX power but are rated as eye-safe according to the authors or are obviously eye-safe due to their setup. The data rates are given for a rough classification but should not be understood as comparable values due to different BER. In addition, our system is not optimized for data rate but maximum dynamic range, i.e., maximum optical amplitude and sensitivity.

C. Future Aspects

The herein used MPL was designed for an industrial application, which uses near-infrared light for communication. It is no problem to fabricate the lens for VLC. However, an interesting topic for further research is the MPL's color mixing property in the case of multiple distinct emitters.

The MPL can be substantially thinner compared to conventional volume lenses if steps are introduced between the facets. This allows cost reduction in high-volume production.

TABLE II

SELECTED LD-BASED LASER CLASS 1/1M OWC LINKS
[1]EXPERIMENTAL, SINGLE CHANNEL; [2]OOK; [3]OFDM

Ref.	Year	Optics	Φ_{TX}	λ	θ	DR^1
			mW	nm	°	Gbit/s
this work	2022	MPL	190	850	7 × 7	1.289[2]
[22]	2021	LD array	130	1550	6	-
[17]	2021	diffusing fiber	-	850	60	≈1.3[3]
[15]	2020	holographic diffuser	170	850	3 × 11	-
[18]	2015	remote phosphor	90	449	60	6.25[3]
[23]	2015	diffuser	20	642	-	4.4[3]
[24]	2010	holographic diffuser	25.1	820	5	1.25[2]
[16]	2010	holographic diffuser	80	860	15	0.28[2]

Due to the freeform nature of the lens, the facets feature typically no symmetry. Therefore, precision milling is required for tool fabrication. Large area lenses result in a rather long tool processing and thus high initial costs.

With the proceeding development of transmitters featuring diffusers, remote phosphor, or MPLs, the eye safety issue of LD transmitters gets more and more solved. The high available power brings up new challenges like the development of laser drivers that are capable of driving LD currents with amplitudes of up to 0.1 A…10 A with a modulation bandwidth in the GHz range. Driver circuits for sub-carrier modulations like OFDM have the additional demand for high linearity. Another challenge is the design of TIAs with ultra-large dynamic range. Taking the sensitivity ($\approx -37\,\mathrm{dBm}$) and the transmitter power ($\approx +23\,\mathrm{dBm}$) of our optical link, we already end up at 60 dB dynamic range. Assuming larger MPLs and LD arrays, the dynamic range will even further increase to 70 dB. Bidirectional, full-duplex links with such a high dynamic range will benefit from multiple access in indoor scenarios because the optical crosstalk between the up- and down-link easily becomes critical due to unintended reflections.

VI. CONCLUSION

This work demonstrates the practical feasibility of MPLs. The MPL is a facetted freeform lens that allows a higher laser power regarding eye safety. The MPL in our setup provides a rectangular emission profile with a half-angle of 7°. It allows for an optical transmitter power of 190 mW while still ensuring laser class 1M. It corresponds to an improvement of 13 dB compared to the same transmitter without MPL. A 1.289 Gbit/s NRZ-OOK PRBS-7 data transfer experiment proves that the MPL does not degrade the transceiver sensitivity. The link with MPL achieves a BER of $\leq 10^{-10}$ for $\Phi_{RX} \geq -31.2\,\mathrm{dBm}$ and $2.4 \cdot 10^{-4}$ for $\Phi_{RX} = -37.3\,\mathrm{dBm}$. The MPL in our optical link enables a range of >5 m, depending on the specified BER. The MPL is suited for optical transceivers with a defined emission profile. It does not limit the data rate in our experiment. Higher data rates can be achieved using higher modulation frequencies or modulation schemes with higher spectral efficiency.

REFERENCES

[1] X. You *et al.*, "Towards 6G wireless communication networks: Vision, enabling technologies, and new paradigm shifts," *Sci. China Inf. Sci.*, vol. 64, no. 1, pp. 1–74, 2021.

[2] P. J. Winzer and D. T. Neilson, "From scaling disparities to integrated parallelism: A decathlon for a decade," *J. Lightw. Technol.*, vol. 35, no. 5, pp. 1099–1115, Mar. 1, 2017.

[3] P. Cerwall. (Jun. 2021). *Ericsson Mobility Report*. Accessed: Jun. 16, 2021. [Online]. Available: https://www.ericsson.com/49cd40/assets/local/mobility-report/documents/2021/june-2021-ericsson-mobility-report.pdf

[4] P. Brandl and H. Zimmermann, "Optoelectronic integrated circuit for indoor optical wireless communication with adjustable beam," in *Proc. 18th Eur. Conf. Netw. Opt. Commun. 8th Conf. Opt. Cabling Infrastruct. (NoC-OC&I)*, Jul. 2013, pp. 149–152.

[5] M. Faulwaser, R. Kirrbach, T. Schneider, and A. Noack, "10 Gbit/s bidirectional transceiver with monolithic optic for rotary connector replacements," in *Proc. Global LIFI Congr. (GLC)*, Feb. 2018, pp. 95–102.

[6] F. Zafar, M. Bakaul, and R. Parthiban, "Laser-diode-based visible light communication: Toward gigabit class communication," *IEEE Commun. Mag.*, vol. 55, no. 2, pp. 144–151, Feb. 2017.

[7] H. Haas, C. Chen, and D. O'Brien, "A guide to wireless networking by light," *Prog. Quantum Electron.*, vol. 55, pp. 88–111, Sep. 2017.

[8] H. Kazemi, E. Sarbazi, M. D. Soltani, M. Safari, and H. Haas, "A Tb/s indoor optical wireless backhaul system using VCSEL arrays," in *Proc. IEEE 31st Annu. Int. Symp. Pers., Indoor Mobile Radio Commun.*, London, U.K., Aug. 2020, pp. 1–6.

[9] *Sicherheit von Lasereinrichtungen—Teil 1: Klassifizierung von Anlagen und Anforderungen*, DIN Deutsches Institut für Normung, Standard DIN EN 60825-1:2015-07, 2015.

[10] *Safety of Laser Products—Part 1: Equipment Classification and Requirements*, International Electrotechnical Commission, Standard IEC 60825-1:2014, 2014.

[11] M. D. Soltani *et al.*, "Safety analysis for laser-based optical wireless communications: A tutorial," 2021, *arXiv:2102.08707*.

[12] M. Faulwasser, F. Deicke, and T. Schneider, "10 Gbit/s bidirectional optical wireless communication module for docking devices," in *Proc. IEEE Globecom Workshops (GC Wkshps)*, Dec. 2014, pp. 512–517.

[13] C. Singh, J. John, Y. N. Singh, and K. K. Tripathi, "Design aspects of high-performance indoor optical wireless transceivers," in *Proc. IEEE Int. Conf. Pers. Wireless Commun. (ICPWC)*, New Delhi, India, Jan. 2005, pp. 14–18.

[14] Z. Wei *et al.*, "Full-duplex high-speed indoor optical wireless communication system based on a micro-LED and VCSEL array," *Opt. Exp.*, vol. 29, no. 3, pp. 3891–3903, 2021.

[15] V. Jungnickel *et al.*, "Laser-based LiFi for 6G: Potential and applications," in *Proc. 9th Laser Display Lighting Conf.* Yokohama, Japan: Pacifico Yokohama, 2020, pp. 166–167.

[16] D. O'Brien *et al.*, "High data-rate infra-red optical wireless communications: Implementation challenges," in *Proc. IEEE Globecom Workshops*, Dec. 2010, pp. 1047–1051.

[17] C. Lee *et al.*, "26 Gbit/s LiFi system with laser-based white light transmitter," *J. Lightw. Technol.*, vol. 40, no. 5, pp. 1432–1439, Mar. 1, 2022.

[18] H. Chun, S. Rajbhandari, D. Tsonev, G. Faulkner, H. Haas, and D. O'Brien, "Visible light communication using laser diode based remote phosphor technique," in *Proc. IEEE Int. Conf. Commun. Workshop (ICCW)*, Jun. 2015, pp. 1392–1397.

[19] R. Kirrbach, T. Schneider, M. Faulwaßer, and K. Zielant, "Multipath lens for eye-safe optical wireless communications," *Opt. Exp.*, vol. 29, no. 19, p. 30208, 2021.

[20] R. Winston, J. C. Miñano, and P. Benítez, *Nonimaging Optics*. Amsterdam, The Netherlands: Elsevier, 2005.

[21] E. Säckinger, *Analysis and Design of Transimpedance Amplifiers for Optical Receivers*. Hoboken, NJ, USA: Wiley, 2017.

[22] Z. Zeng, M. D. Soltani, M. Safari, and H. Haas, "A VCSEL array transmission system with novel beam activation mechanisms," *IEEE Trans. Commun.*, vol. 70, no. 3, pp. 1886–1900, Mar. 2022.

[23] B. Janjua *et al.*, "Going beyond 4 Gbps data rate by employing RGB laser diodes for visible light communication," *Opt. Exp.*, vol. 23, no. 14, pp. 18746–18753, 2015.

[24] H. Le Minh, D. O'Brien, and G. Faulkner, "A Gigabit/s indoor optical wireless system for home access networks," in *Proc. 7th Int. Symp. Commun. Syst., Netw. Digit. Signal Process. (CSNDSP)*, Newcastle Upon Tyne, U.K., Jul. 2010, pp. 532–536.